Macromolecules

Article

Cite This: Macromolecules 2018, 51, 5798−5805

pubs.acs.org/Macromolecules

Hydrogel Microcapsules with Dynamic pH-Responsive Properties from Methacrylic Anhydride

Jörg G. Werner,[†] Saraf Nawar,[†] Alexander A. Solovev,[†,§] and David A. Weitz*[,†,‡]

[†]John A. Paulson School of Engineering and Applied Sciences and [‡]Department of Physics, Harvard University, Cambridge, Massachusetts 02138, United States

[§]Department of Materials Science, Fudan University, Shanghai, P. R. China

Supporting Information

ABSTRACT: Dynamic microcapsules are a highly sought-after class of encapsulant for advanced delivery applications with dynamically tunable release profiles, as actively manipulatable microreactors, or as selective microtraps for molecular separation and purification. Such dynamic microcapsules can only be realized with a nondestructive trigger-response mechanism that changes the permeability of the shell membrane reversibly, as found in hydrogels. However, the direct synthesis of a trigger-responsive hydrogel membrane around a water drop without the use of sacrificial templates remains elusive due to the incompatibility of the synthesis chemistry with aqueous emulsion processing. Here, we report on a facile approach to fabricate reversibly responsive hydrogel microcapsules utilizing reactive anhydride chemistry. Cross-linked and hydrophobic poly(methacrylic anhydride) microcapsules are obtained from microfluidic double emulsion drop templating that enables direct encapsulation of hydrophilic, water-suspended cargo within the aqueous core. Hydrolysis in aqueous environment yields microcapsules with a poly(acid) hydrogel shell that exhibit high mechanical and chemical stability for repeated cycling between its swollen and nonswollen states without rupture or fatigue. The permeability of the microcapsules is strongly dependent on the degree of swelling and hence can be actively and dynamically modified, enabling repeated capture, trap, and release of aqueous cargo over numerous cycles.

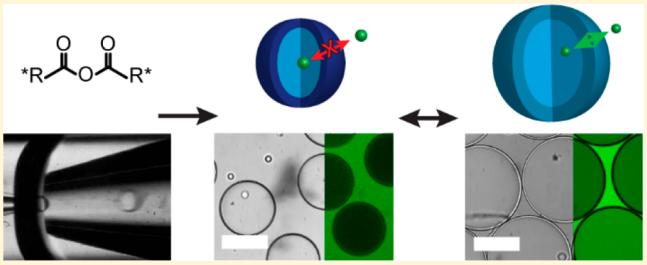

INTRODUCTION

Microcapsules are widely employed for encapsulation, protection, and release of sensitive actives in areas such as drug delivery, cosmetics, agriculture, and food additives.[1−4] Common architectures contain the dispersed or dissolved cargo in an aqueous core that is surrounded by a polymeric membrane. Release mechanisms involve either diffusion of the active substance through the membrane or shell disintegration and rupture.[5−8] Numerous single-use capsule systems have been developed to control the release onset and rate in response to trigger events such as shear, light, and changes in pH, temperature, or redox potentials.[9−14] Microcapsules with reversibly responsive shells that act as a gatekeeper would enable on−off release in which diffusion is turned off when the release trigger is reversed. The aqueous core of such dynamic capsule systems could be loaded numerous times with cargo substances making reuse and recycling of microcapsules over multiple cycles possible. Furthermore, dynamic microcapsules could act as a probe that selectively collects molecular substances from aqueous environments at predetermined conditions and trap them by shutting off its shell's permeability for subsequent examination, processing, or release, enabling new ways of molecular analysis and purification. However, due to the destructive and irreversible nature of the commonly employed release mechanisms, no aqueous microcapsule systems have been reported that address its reversal, namely turning release off nondistructively.[15−17] A trigger-responsive mechanism that alters the shell's permeability reversibly and nondestructively is necessary to shut off diffusion at any time and hence interrupt release or uptake. The lack of methods for the fabrication of water-cored capsules dispersed in aqueous media with membranes that allow for dynamic permeability changes is due to the solubility of their molecular precursors, making sacrificial templates necessary as a placeholder for the aqueous microreactor, which precludes direct encapsulation of functional actives.[18−22]

Here we report the synthesis of microcapsules containing a shell with reversibly tunable permeation that acts as a gatekeeper for controlled diffusion in and out of the aqueous core. The membrane is composed of a pH-responsive hydrogel that significantly and reversibly changes its permeability to macromolecular species upon changes in pH. To be able to synthesize a hydrogel membrane directly around a water core, we employ anhydride chemistry in combination with complex emulsion drop templating.[23−25] The reversibly responsive hydrogel membrane allows fast diffusion in and out of the

Received: April 20, 2018
Revised: July 3, 2018
Published: July 24, 2018

DOI: 10.1021/acs.macromol.8b00843
Macromolecules 2018, 51, 5798−5805

Scheme 1. Conversion of Water-in-Oil-in-Water Double Emulsion Drop with Monomer Shell to Poly(anhydride) Microcapsules and Subsequent Hydrolysis to Cross-Linked Poly(acid) Microcapsules

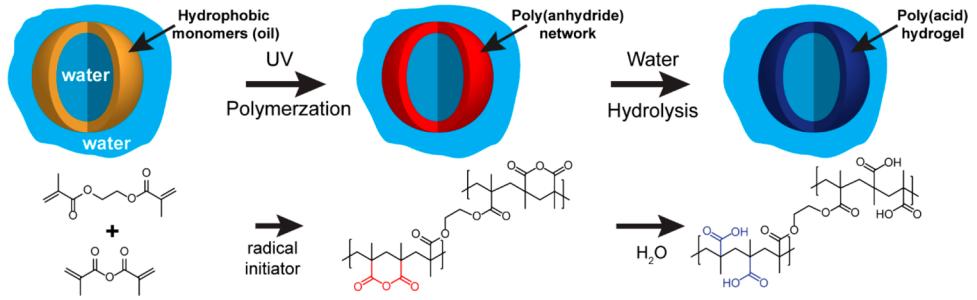

water droplet when swollen in neutral and alkaline conditions, while permeability is shut off upon deswelling in acidic conditions. Significantly, the process is reversible, allowing dynamic on- and off-switching of supply and release of molecular species in response to pH changes over multiple cycles without sacrificing the structural integrity of the microcapsule.

EXPERIMENTAL METHODS

Hydrophobic monomer mixtures of methacrylic anhydride (MAAn) and ethylene glycol dimethacrylate (EGDMA) containing either 96.1 or 81.8 mol % of MAAn are prepared, degassed, and combined with the radical photoinitiator 2-hydroxy-2-methylpropiophenone (Darocure 1173) at 1 mol %. The monomer mixture is used as the shell phase in water-in-oil-in-water double emulsion drops without any solvent. Microcapsules are produced from double emulsion drops with an aqueous core containing 5 wt % poly(vinyl alcohol) (PVA, M_w 13 000−23 000, 98% hydrolyzed) as stabilizer. The drops are dispersed in an aqueous continuous phase also containing 5 wt % PVA. Water-in-oil-in-water double emulsions are fabricated using a glass capillary microfluidic device.[26,27] The device consists of two tapered cylindrical capillaries aligned inside a square capillary with inner dimensions slightly larger (1.05 mm) than that of the outer diameter of the cylindrical capillaries (1 mm). The injection capillary is rendered hydrophobic by treating it with octadecyltrimethoxysilane. The collection capillary is rendered hydrophilic by treating with 2-(methoxy(polyethyleneoxy)propyl)trimethoxysilane. The inner aqueous phase is injected through the inside of the hydrophobically treated injection capillary, the middle shell phase is injected from the same direction through the interstitial space between the square capillary and the injection capillary, and the outer aqueous phase is injected from the opposite direction through the interstitial space between the square capillary and collection capillary. Drop formation in the glass capillary device is monitored with a fast camera (Phantom V9.0) equipped onto a Leica inverted optical microscope. Double emulsion drops are formed in the dripping regime at flow rates of 1000, 250, and 25 000 μL h^{-1} for the inner, middle, and outer phases, respectively. The double emulsion drops are immediately irradiated with UV light (OmiCure S1500, 320−500 nm filter) to photopolymerize the shells at the end of the outlet capillary. The microcapsules are collected and washed with deionized water.

The poly(methacrylic anhydride-*co*-ethylene glycol dimethacrylate) microcapsules are hydrolyzed in various buffer solutions or in DI water. Microcapsule hydrolysis, permeability, and molecular weight cutoff (MWCO) of the poly(methacrylic acid-*co*-ethylene glycol dimethacrylate) hydrogel shells under various pH conditions are characterized using molecular permeation into the capsule interior of sulforhodamine B (0.1 mg mL^{-1}) or rhodamine- and fluorescein-conjugated dextrans (1 mg mL^{-1}) of known molecular weight (Sigma) in aqueous solution. Osmotic shock response is measured with 200 g L^{-1} solutions of sucrose and γ-cyclodextrin (γ-CD) that are added to aliquots of microcapsules in various buffer solutions. Swelling cycles of hydrogel microcapsules are performed by alternating exposure to 0.02 M acetate buffer (pH = 4) and 0.02 M sodium phosphate buffer (pH = 7), removing the supernatant before every new addition. Capture, trap, and release experiments are performed similarly with fluorescently labeled dextran added to the initial alkaline buffer. All buffers were BDH pH Reference Standard Buffers except for the osmotic shock and pH cycling experiments, which were prepared as 0.02 M solutions at appropriate ratios of acetic acid and sodium hydroxide for pH 4 and sodium phosphate mono- and dibasic for pH 7.

Hydrolysis, dye-conjugate diffusion, time-resolved swelling cycles, and capture, trap, and release of the fluorescent probe are characterized and monitored with a laser confocal fluorescence microscope (Leica Microsystems TCS SP5) using 488 or 543 nm for the excitation and 490−520 nm or 560−620 nm for fluorescence detection of fluorescein- or rhodamine-containing fluorophores, respectively. For hydrolysis and permeability characterization, an aliquot of 30−40 μL of the microcapsule dispersion containing around 60−100 capsules is transferred into wells of a 96-well plate and combined with 100 μL of the respective buffer solutions. Subsequently, 20 μL of the fluorophore solution or sugar solution is added to the well. Small aliquots of capsules for FT-IR characterization are washed four times with DI water and dried under vacuum. Measurements are performed using a Bruker FT-IR microscope (Lumos) in attenuated total reflectance (ATR) mode. Scanning electron microscopy (SEM) samples are prepared the same way as for FT-IR, and imaging is performed on a field emission scanning electron microscope (FESEM, Zeiss Supra55VP) equipped with an in-lens detector at an accelerating voltage of 3 kV.

RESULTS AND DISCUSSION

Water-immiscible methacrylic anhydride (MAAn) is employed as the source for the pH-responsive poly(methacrylic acid) hydrogel that is cross-linked with ethylene glycol dimethacrylate (EGDMA), as illustrated in Scheme 1. The copolymerization of MAAn and EGDMA as the shell phase in W/O/W double emulsion drops yields hydrophobic poly(methacrylic anhydride-*co*-ethylene glycol dimethacrylate) (P(MAAn−EGDMA)) microcapsules filled with and surrounded by water. Upon simple hydrolysis in their aqueous environment, each of the anhydride groups in the polymerized shell is converted into two methacrylic acid groups with a rate depending on pH and cross-link density, yielding an EGDMA-cross-linked poly(methacrylic acid) hydrogel shell. The polymerization of a W/O/W double emulsion drop to a hydrophobic polymer microcapsule and its conversion to a water-cored hydrogel microcapsule is illustrated in Scheme 1. The weak acidity of the cross-linked poly(methacrylic acid) hydrogel shells renders the microcapsules reversibly pH-responsive.

Water-in-oil-in-water double emulsion drops are fabricated using glass capillary microfluidics.[26,27] The microfluidic production of double emulsion drops enables the fabrication

DOI: 10.1021/acs.macromol.8b00843
Macromolecules 2018, 51, 5798−5805

of microcapsules with a high degree of control over structural features such as diameter and shell thickness combined with virtually quantitative encapsulation efficiency of active substances inside the aqueous core.[26,28] The device consists of two tapered cylindrical capillaries aligned inside a square capillary with dimensions slightly larger than that of the outer diameter of the cylindrical capillaries. To form double emulsions, the inner aqueous phase is injected through the hydrophobically treated injection capillary, while the middle shell phase consisting of the hydrophobic monomer mixture and a radical photoinitiator is injected from the same direction through the interstitial space between the square capillary and the injection capillary, as illustrated in Figure 1a. The outer

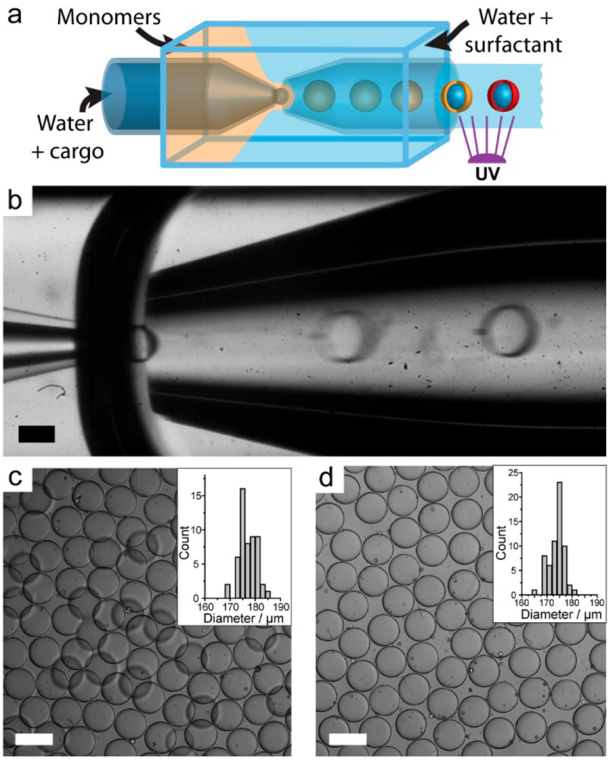

Figure 1. (a) Schematic of double emulsion drop formation and microcapsule fabrication in a microfluidic glass capillary device. (b–d) Light microscopy images of methacrylic anhydride double emulsion drop formation in a microfluidic glass capillary device (b) and resulting cross-linked poly(methacrylic anhydride-*co*-ethylene glycol dimethacrylate) (P(MAAn–EGDMA)) microcapsules with 96.1 mol % (c) and 81.8 mol % (d) methacrylic anhydride. Scale bars are 200 μm. Insets in (c) and (d) show histograms of the capsule diameters.

aqueous phase is injected from the opposite direction, through the interstitial space between the square capillary and collection capillary. At the tip of the injection capillary, the inner phase and the surrounding middle monomer phase are hydrodynamically focused by the outer phase; the coaxial stream of fluids breaks up to form double emulsion drops, as shown in Figure 1a,b and Video SV1. Following formation, the double emulsion drops flow through the cylindrical collection capillary and are immediately irradiated with UV light to photopolymerize the shells. The poly(anhydride) microcapsules exhibit very low size dispersity of less than 2% deviation, as shown by the optical microscopy images in Figure 1c,d and summarized in Table S1.

Hydrophilic microcapsules with poly(acid) hydrogel shells are obtained through hydrolysis of the poly(anhydride) microcapsules. The poly(methacrylic anhydride-*co*-ethylene glycol dimethacrylate) shells are hydrolyzed under various pH conditions to study the effect of pH on the hydrolysis rate. During hydrolysis, the anhydride units of the polymerized microcapsule shell are cleaved to yield tethered carboxylic acid groups, increasing the hydrophilicity of the shell. The enhanced hydrophilicity of the shell membrane increases water content and allows the diffusion of small hydrophilic molecules into the microcapsule core. The completion of hydrolysis of the poly(anhydride) network is indicated by the diffusion of the hydrophilic dye sulforhodamine B into the capsule interior, monitored by fluorescence confocal microscopy. The hydrolysis rate increases with the alkalinity of the aqueous medium, as shown in Figure 2a and Figure S1. For microcapsules containing 3.9 mol % EGDMA cross-linker, the shells are fully hydrolyzed after 1 day at pH 11. For microcapsules at pH 7, hydrolysis takes longer, and microcapsules show fluorescent interiors only after 6 days. In more acidic environments, the time required for hydrolysis further increases to 11 and 13 days for microcapsules in DI water and at pH 2, respectively, as shown in Figure 2a and Figure S1. This trend is expected, given that at pH conditions below the pK_a of poly(methacrylic acid), the hydrolyzed carboxylic acid groups are protonated, which lowers the hydrophilicity of the converting microcapsule shell, thus requiring longer for the conversion of the poly(anhydride) network to a poly(acid) network. Regardless of environmental pH conditions, microcapsules remain intact without degradation or rupturing of the shell. Hydrolysis of the poly(anhydride) capsules is further confirmed using Fourier transform infrared spectroscopy (FT-IR). Hydrolyzed microcapsules show the presence of a broad, prominent absorption band at wavenumbers of 3000–3500 cm^{-1} corresponding to the introduced hydroxyl groups. This OH-stretching band is absent in the poly(anhydride) microcapsules before hydrolysis, as shown in the ATR-FT-IR spectra in Figure 2b. Interestingly, the commonly observed absorption peak for poly(methacrylic anhydride) at 1800 cm^{-1} is only present in the FT-IR spectrum of the microcapsules with 81.8% MAAn before hydrolysis.[29] We assume that the faster hydrolysis rate of the microcapsules with higher anhydride content and lower cross-link density leads to partial hydrolysis of the surface layer of the polymer shells during the washing and drying before FT-IR measurements, causing the disappearance of this peak for those capsules. The shell maintains its homogeneous structure following hydrolysis with a thickness of a few micrometers both before and after hydrolysis, as shown by the scanning electron microscopy images of microcapsule cross sections in Figure 2c.

While the polymerized anhydride serves as the precursor to the stimuli-responsive poly(acid), the permanent cross-linker EGDMA ensures the structural integrity of the microcapsules during the hydrolysis process and determines the cross-link density of the dynamic hydrogel shell. Hydrolysis is slower for poly(anhydride) microcapsules with a higher cross-link density of 18.2 mol % EGDMA, but the effect of pH on the hydrolysis rate remains the same, as shown in Figure S1b. The higher concentration of EGDMA cross-linker in the shell leads to lower swelling capacity upon hydrolysis, which decreases the amount of water at the hydrolysis front and thus lowers its rate. While methacrylic anhydride can form a partially cross-linked polymer network by itself and microcapsules are obtained

DOI: 10.1021/acs.macromol.8b00843
Macromolecules 2018, 51, 5798–5805

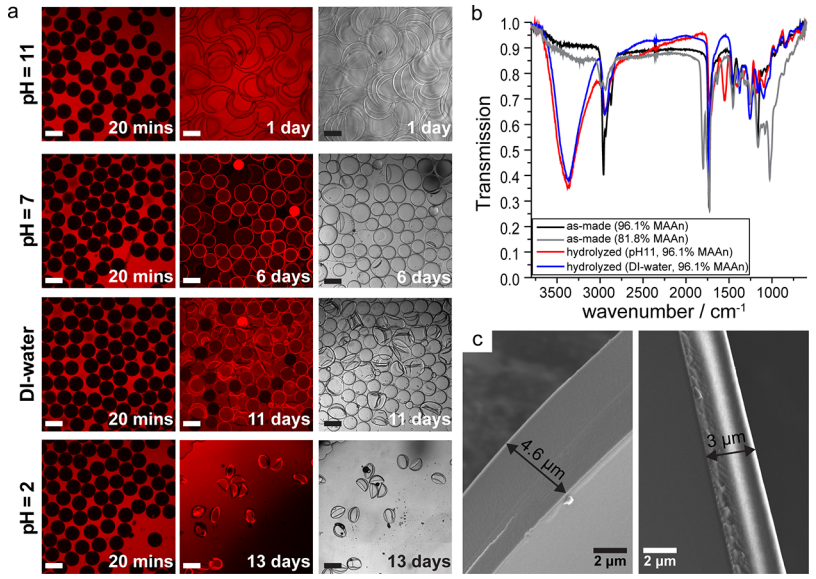

Figure 2. (a) Fluorescence confocal laser microscopy images before (left) and after (middle) hydrolysis of poly(methacrylic anhydride-*co*-ethylene glycol dimethacrylate) microcapsules with 96.1 mol % methacrylic anhydride in various pH environments. The capsules were challenged with the fluorescent probe sulforhodamine B. Bright-field microscopy image of the hydrolyzed poly(methacrylic acid-*co*-ethylene glycol dimethacrylate) microcapsules (right). All scale bars are 200 μm. (b) ATR-FT-IR spectra of selected microcapsules before and after hydrolysis in various conditions. (c) Scanning electron microscopy images of the shell cross section of microcapsules with 96.1 mol % methacrylic anhydride before (left) and after (right) hydrolysis at pH = 7.

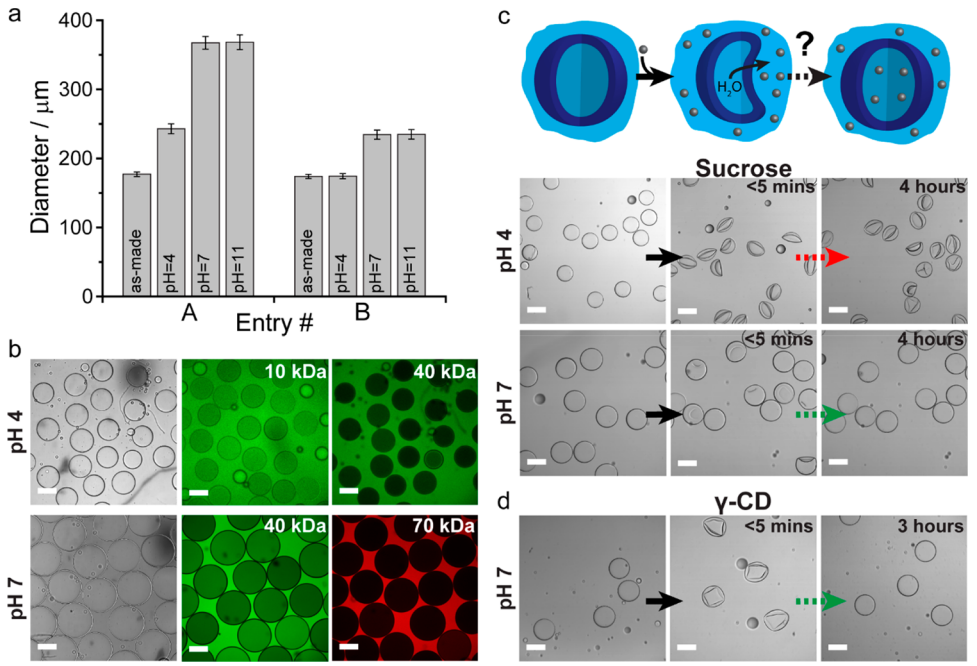

Figure 3. (a) Diameters of P(MAA−EGDMA) microcapsules with 98 mol % (A) and 90 mol % (B) acid content assuming full hydrolysis of all anhydride units from initially 96.1% and 81.8% anhydride, respectively, before (as-made) and after hydrolysis at various pH. Values and error bars represent geometric average and standard deviation of at least 18 capsules. (b) Bright-field (left) and fluorescence confocal (middle, right) micrographs of P(MAA-EGDMA) microcapsules with 98 mol % acid content challenged with fluorescently labeled dextran molecules with indicated molecular weight at indicated pH (same pH in same row). (c, d) Schematic illustration of the osmotic shock experiment to characterize the shell's permeability to small molecular solutes (c, top row) and bright-field microscopy images of P(MAA−EGDMA) microcapsules with 90 mol % acid content before (left) and after (middle, right) being challenged with sucrose (c) or γ-cyclodextrin (γ-CD) (d) solution at indicated pH. All scale bars are 200 μm.

without the addition of the permanent cross-linker EGDMA, they completely dissolve upon hydrolysis, as expected for linear poly(methacrylic acid) macromolecules in aqueous environment. This observation additionally supports the assumption of full hydrolysis of all methacrylic anhydride units over time. Our results demonstrate that the hydrolysis rate of the microcapsule shell is strongly dependent on the pH of the microcapsules' environment and the cross-link density of the shell. As such, tuning the molecular composition of the microcapsule shell

DOI: 10.1021/acs.macromol.8b00843
Macromolecules 2018, 51, 5798−5805

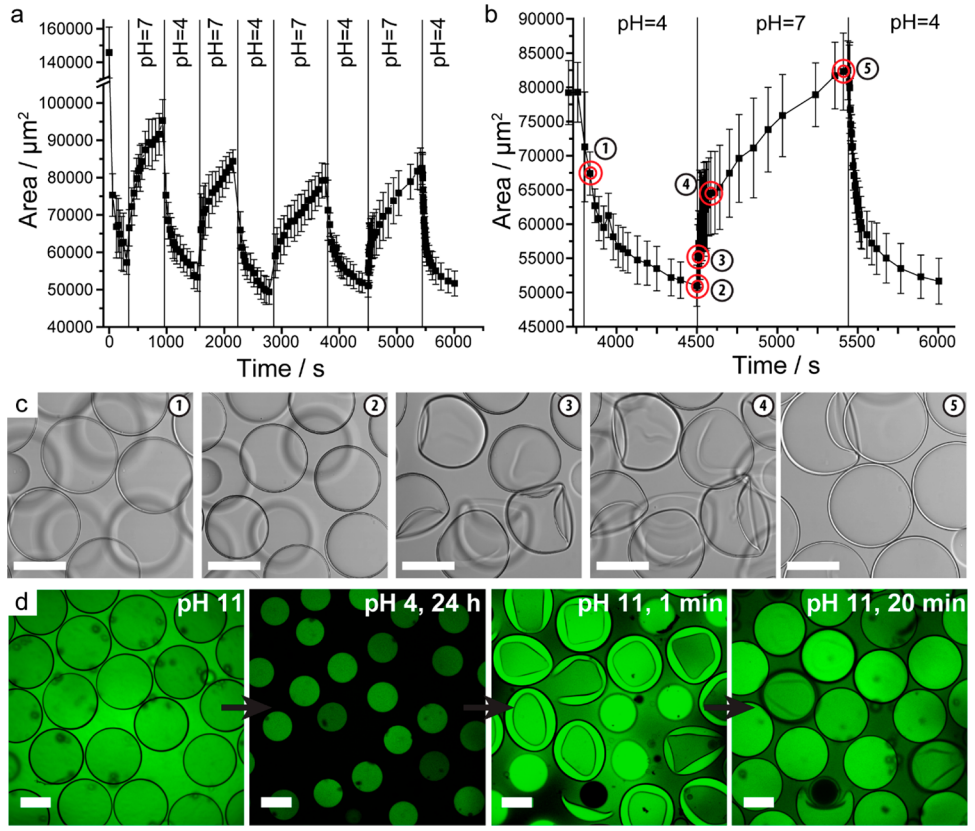

Figure 4. (a, b) Time-resolved size distribution (projected area) of the cyclic swelling (pH = 7) and deswelling (pH = 4) of P(MAA−EGDMA) hydrogel microcapsules with 98 mol % acid content. Droplines represent time of pH change. (c) Selected bright-field microscopy images of the P(MAA−EGMDA) microcapsules during swelling and deswelling at the indicated time points in plot (b). (d) Fluorescence confocal laser micrographs of P(MAA−EGDMA) microcapsules with 98 mol % acid content during a capture−trap−release cycle of fluorescently labeled dextran with a molecular weight of 20 kDa at indicated pH and time after pH change. All scale bars are 200 μm.

provides a viable approach for controlling hydrolysis in a given environment and, consequently, release onset time.

After hydrolysis of the anhydrides, the microcapsule shells are composed of a cross-linked poly(methacrylic acid) hydrogel. The weak acidity of the methacrylic acid units renders the hydrogel microcapsules reversibly responsive to changes in pH. Above its pK_a, the poly(acid) network is charged due to the deprotonation of the methacrylic acid, causing the hydrogel shells to swell significantly with water. At pH values below the pK_a, protonation of the methacrylic acid groups causes hydrogen bonding within the uncharged polymer network, collapsing and deswelling the hydrogel shells. The pK_a of poly(methacrylic acid) is around 6, with some dependence on the molecular and ionic environment.[30−32] Hence, the degree of swelling of the hydrogel shell, and thus the size of the microcapsules, depends on the pH of the aqueous environment. Poly(methacrylic acid) microcapsules with 2 mol % cross-links have a diameter of 243 ± 7 μm at pH 4 and grow to 367 ± 9 and 368 ± 11 μm upon pH increase to 7 and 11, respectively, as shown in Figure 3a,b. The size difference between low and high pH corresponds to 51% in diameter and 240% in microcapsule volume. The degree of deprotonation well above the pK_a of the poly(acid) network is very similar, causing the similarity in size between microcapsules in neutral and alkaline conditions.[33−35] Despite the significant difference in size between various conditions, the size dispersity remains low, in both the swollen and nonswollen states. The increase in capsule size is not predominantly driven by an increase in shell thickness but is caused by the in-plane expansion of the hydrogel shell due to the water swelling, significantly increasing the capsule's surface area. For example, in the thin shell limit, if the shell of a microcapsule with a diameter 180 μm and a shell thickness of 4 μm doubles in volume homogeneously in all directions, the shell thickness only increases by 1 μm, but the surface area of the microcapsule increases by 59%, leading to a microcapsule diameter change of 46 μm, similarly to what we observe for our microcapsules with 10% cross-link density. Thus, the core volume simply changes to accommodate the difference in capsule surface area imposed by the degree of swelling of the hydrogel shell. This is in stark contrast to microgels that swell homogeneously throughout the entire hydrogel microparticle. The degree of swelling of the poly(acid) hydrogel shells impacts the microcapsules' permeability. The molecular weight cutoff (MWCO), the threshold weight of molecules that can diffuse through the shell, increases with higher degree of swelling. At pH 4, microcapsules with 2 mol % cross-linker exhibit permeability to dextran molecules with a molecular weight of 10 kg mol^{-1} but are impermeable to 40 kg mol^{-1} dextran. At pH 7, the same microcapsules are permeable to dextran with molecular weights up to 40 kg mol^{-1}, demonstrating the pH-dependent permeability and MWCO of the hydrogel microcapsules, as shown in the fluorescence confocal microscopy images in Figure 3b. In the swollen state, the capsules are still impermeable to larger dextran of 70 kg mol^{-1}, indicating the structural integrity of the shells without

DOI: 10.1021/acs.macromol.8b00843
Macromolecules 2018, 51, 5798−5805

defects or rupture. Higher cross-link density lowers the swelling capacity of hydrogels. Microcapsules with 10 mol % cross-links exhibit a diameter of 174 ± 4 and 234 ± 7 μm at pH 4 and 7, respectively, a 34% difference as summarized in Figure 3a. The highly cross-linked microcapsules are impermeable to dextran with molecular weights down to 4 kg mol^{-1} at any pH. Thus, to assess their permeability, these highly cross-linked hydrogel microcapsules are osmotically challenged with sucrose and γ-cyclodextrin (γ-CD) at pHs of 4 and 7. Increasing the concentration of a solute in the continuous phase increases its osmolarity, leading to water diffusion from the microcapsule core to the water phase outside the microcapsules. The egress of water from the microcapsule core causes the shells to buckle. If the solute is able to permeate through the shell into the core, the microcapsules unbuckle over time, as schematically shown in Figure 3c. The lower the permeability of the shell to the solute, the longer it takes for the microcapsule to return to its spherical shape. The poly(methacrylic acid) microcapsules with 10 mol % cross-linker buckle significantly when sucrose is added to the continuous phase at pH 4 and remain buckled. At pH 7, these capsules only buckle slightly immediately after adding sucrose but quickly return to the spherical shape, indicating good permeability of the shells to sucrose at pH 7, and low permeability at pH 4, as shown in Figure 3c. γ-CD causes the capsules to buckle significantly upon its addition to the continuous aqueous phase at pH 7, but the microcapsules regain their spherical shape within hours, indicating permeability of the microcapsules to the larger sugar with a lower diffusion rate. Time-resolved optical microscopy images of the osmotic shock experiments demonstrating the pH-dependent permeability of the small sugar molecules are shown in Figure 3c,d.

The pH-triggered change in size and permeability of the hydrogel microcapsules is repeatable, enabled by the reversible swelling mechanism through protonation. Thus, the microcapsules can be repeatedly cycled between their swollen and nonswollen states. These dynamic properties are investigated by measuring the size of the microcapsules with 2 mol % cross-linker under alternating pH conditions above and below the pK_a of the poly(acid) network. The swelling and deswelling of the pH-responsive microcapsules are fast and reversible, with no sign of structural deterioration observed over five cycles, as shown in Figure 4a,b. The capsule size, measured as projected area, changes exponentially after each pH switch over the course of minutes. The projected microcapsule area is not indicative of the shell size after the switch to pH = 7 due to a change in shape during the swelling process: upon pH increase from 4 to 7, the shells swell predominantly in plane, leading to a significant increase of the microcapsules surface area. The diffusion of water through the shell into the core is too slow to accommodate this increased surface area immediately; this results in buckling of the microcapsules. Additionally, the capsules are not allowed to fully equilibrate their size after each trigger event in this demonstration. Hence, the response of the microcapsules depends on their swelling history and is not expected to be exactly the same in each cycle. The capsules become fully spherical again after approximately 15 min when the core is filled with sufficient water volume, as shown in Figure 4c. The early stages of the microcapsule shape transition and size increase upon pH change from 4 to 7 are shown in Video SV2.

Deswelling of the microcapsules is initiated by a drop in pH to 4, below the pK_a of the hydrogel shell. During this process, the cross-linked poly(methacrylic acid) hydrogel membrane is protonated, yielding lower water-swelling capacity. The expulsion of water from the microcapsule shell causes its shrinking and accordingly a decrease of the microcapsule surface area that is accommodated by a reduction of core volume. The reduction of core volume proceeds by the diffusion of water through the deswollen shell, slowing down the decrease of microcapsule size. Significantly, the microcapsule shells do not rupture during this shrinking process, enabling repeated swelling and deswelling. The shrinking of the microcapsules upon pH change from 7 to 4 is shown in Video SV3. Overall, no sign of structural failure or fatigue is observed during the cyclic swelling, buckling, and deswelling processes, suggesting suitable mechanical stability of the pH-responsive hydrogel microcapsules for their repeated utilization as dynamic microcarriers of liquid cargo. Furthermore, the dynamically responsive poly(acid) microcapsules exhibit good hydrolytic stability: after one year of storage in water at room temperature no degradation is observed, as shown in Figure S2. Even in harsh conditions such as 1 M hydrochloric acid and 1 M sodium hydroxide the capsules show no sign of degradation over at least 9 days.

The dynamically tunable swelling and permeability of the pH-responsive microcapsules are utilized to capture, trap, and release appropriately sized molecular species. Microcapsules with 2 mol % cross-link density are permeable to dextran with a molecular weight of 20 kDa in the swollen state but impermeable to the same molecule in an acidic environment. When challenged with fluorescently labeled 20 kDa dextran in alkaline conditions, the microcapsules capture the probe molecule, as shown in the leftmost panel of Figure 4d. Upon transfer to acidic medium with a pH of 4, the decrease of the MWCO causes the 20 kDa dextran to be trapped within the core of the microcapsules without observable leakage of the fluorescent probe into the surrounding continuous medium over 24 h. Immediately upon pH increase and microcapsule swelling, the 20 kDa dextran is released from the pH-responsive microcapsules. Fluorescence confocal microscopy images at the respective stages of a capture−trap−release cycle of fluorescently labeled 20 kDa dextran are shown in Figure 4d.

CONCLUSION

In this report, we demonstrate the successful synthesis of water-cored hydrogel microcapsules with reversible trigger-responsiveness without the use of sacrificial templates. We employ hydrophobic anhydride-containing monomers as the shell of double emulsion drops for the direct microfluidic production of polymeric microcapsules, which subsequently convert to poly(methacrylic acid) hydrogel-shelled capsules with tunable conversion time. The template-free synthesis enables the direct encapsulation of large cargo such as catalyst particles in the aqueous core-compartment surrounded by a trigger-responsive hydrogel membrane, as shown in Figure S3. The hydrogel microcapsules exhibit swelling and permeability dependent on cross-link density and pH conditions. Most importantly, the permeability and size of the microcapsules are dynamically tunable over multiple cycles by changing the pH around the microcapsules with retention of their structural integrity. The dynamically triggerable permeability changes allow the microcapsules to be employed as active delivery vehicles that can stop their release after initiation or that can be

DOI: 10.1021/acs.macromol.8b00843
Macromolecules 2018, 51, 5798−5805

recycled as well as repeatedly loaded. Hence, the dynamic microcapsules could be used as an injectable and self-adapting drug reservoir to release hydrophilic actives only in physiological conditions. Additionally, the reversibly responsive microcapsules can be utilized as collection microtraps to capture molecules selectively in neutral or alkaline conditions for subsequent analysis or processing, but not in acidic environments. Such a collection probe could capture molecules such as enzymes selectively from nonacidic areas within the intestinal tract and block the uptake of molecules in the acidic stomach while passing through the digestive system.

■ ASSOCIATED CONTENT

Supporting Information

The Supporting Information is available free of charge on the ACS Publications website at DOI: 10.1021/acs.macromol.8b00843.

Experimental details, Table S1, Figures S1−S3 (PDF)
Video SV1 showing droplet generation (AVI)
Video SV2 showing pH triggered capsule swelling (AVI)
Video SV3 showing pH triggered capsule deswelling (AVI)

■ AUTHOR INFORMATION

Corresponding Author

*(D.A.W.) E-mail weitz@seas.harvard.edu.

ORCID

Jörg G. Werner: 0000-0001-7845-086X
David A. Weitz: 0000-0001-6678-5208

Author Contributions

J.G.W. and S.N. contributed equally. All authors have given approval to the final version of the manuscript.

Notes

The authors declare no competing financial interest.

■ ACKNOWLEDGMENTS

This work was supported by the National Science Foundation (DMR-1708729). This work was performed in part at the Center for Nanoscale Systems (CNS), a member of the National Nanotechnology Coordinated Infrastructure Network (NNCI), which is supported by the National Science Foundation under NSF Award No. 1541959. CNS is part of Harvard University.

■ REFERENCES

(1) Pessi, J.; Santos, H. A.; Miroshnyk, I.; Joukoyliruusi; Weitz, D. A.; Mirza, S. Microfluidics-Assisted Engineering of Polymeric Microcapsules with High Encapsulation Efficiency for Protein Drug Delivery. *Int. J. Pharm.* **2014**, *472* (1−2), 82−87.

(2) Lee, H.; Choi, C.-H.; Abbaspourrad, A.; Wesner, C.; Caggioni, M.; Zhu, T.; Weitz, D. A. Encapsulation and Enhanced Retention of Fragrance in Polymer Microcapsules. *ACS Appl. Mater. Interfaces* **2016**, *8* (6), 4007−4013.

(3) John, R. P.; Tyagi, R. D.; Brar, S. K.; Surampalli, R. Y.; Prévost, D. Bio-Encapsulation of Microbial Cells for Targeted Agricultural Delivery. *Crit. Rev. Biotechnol.* **2011**, *31* (3), 211−226.

(4) Bakry, A. M.; Abbas, S.; Ali, B.; Majeed, H.; Abouelwafa, M. Y.; Mousa, A.; Liang, L. Microencapsulation of Oils: A Comprehensive Review of Benefits, Techniques, and Applications. *Compr. Rev. Food Sci. Food Saf.* **2016**, *15* (1), 143−182.

(5) Kim, M.; Yeo, S. J.; Highley, C. B.; Burdick, J. A.; Yoo, P. J.; Doh, J.; Lee, D. One-Step Generation of Multifunctional Polyelectrolyte Microcapsules *via* Nanoscale Interfacial Complexation in Emulsion (NICE). *ACS Nano* **2015**, *9* (8), 8269−8278.

(6) Amato, D. V.; Lee, H.; Werner, J. G.; Weitz, D. A.; Patton, D. L. Functional Microcapsules via Thiol−Ene Photopolymerization in Droplet-Based Microfluidics. *ACS Appl. Mater. Interfaces* **2017**, *9* (4), 3288−3293.

(7) Seiffert, S.; Thiele, J.; Abate, A. R.; Weitz, D. A. Smart Microgel Capsules from Macromolecular Precursors. *J. Am. Chem. Soc.* **2010**, *132* (18), 6606−6609.

(8) Siltanen, C.; Diakatou, M.; Lowen, J.; Haque, A.; Rahimian, A.; Stybayeva, G.; Revzin, A. One Step Fabrication of Hydrogel Microcapsules with Hollow Core for Assembly and Cultivation of Hepatocyte Spheroids. *Acta Biomater.* **2017**, *50*, 428−436.

(9) Bédard, M. F.; De Geest, B. G.; Skirtach, A. G.; Möhwald, H.; Sukhorukov, G. B. Polymeric Microcapsules with Light Responsive Properties for Encapsulation and Release. *Adv. Colloid Interface Sci.* **2010**, *158* (1−2), 2−14.

(10) Huang, F.; Liao, W. C.; Sohn, Y. S.; Nechushtai, R.; Lu, C. H.; Willner, I. Light-Responsive and pH-Responsive DNA Microcapsules for Controlled Release of Loads. *J. Am. Chem. Soc.* **2016**, *138* (28), 8936−8945.

(11) Wang, Z.; Gao, J.; Ustach, V.; Li, C.; Sun, S.; Hu, S.; Faller, R. Tunable Permeability of Cross-Linked Microcapsules from pH-Responsive Amphiphilic Diblock Copolymers: A Dissipative Particle Dynamics Study. *Langmuir* **2017**, *33* (29), 7288−7297.

(12) Trongsatitkul, T.; Budhlall, B. M. Multicore-Shell PNIPAm-Co-PEGMa Microcapsules for Cell Encapsulation. *Langmuir* **2011**, *27* (22), 13468−13480.

(13) Li, Z.; Liu, S.; Wang, S.; Qiang, L.; Yang, T.; Wang, H.; Möhwald, H.; Cui, X. Synthesis of Folic Acid Functionalized Redox-Responsive Magnetic Proteinous Microcapsules for Targeted Drug Delivery. *J. Colloid Interface Sci.* **2015**, *450*, 325−331.

(14) Chen, P. W.; Erb, R. M.; Studart, A. R. Designer Polymer-Based Microcapsules Made Using Microfluidics. *Langmuir* **2012**, *28* (1), 144−152.

(15) Abbaspourrad, A.; Carroll, N. J.; Kim, S. H.; Weitz, D. A. Polymer Microcapsules with Programmable Active Release. *J. Am. Chem. Soc.* **2013**, *135* (20), 7744−7750.

(16) Grolman, J. M.; Inci, B.; Moore, J. S. pH-Dependent Switchable Permeability from Core−Shell Microcapsules. *ACS Macro Lett.* **2015**, *4* (4), 441−445.

(17) Tang, S.; Tang, L.; Lu, X.; Liu, H.; Moore, J. S. Programmable Payload Release from Transient Polymer Microcapsules Triggered by a Specific Ion Coactivation Effect. *J. Am. Chem. Soc.* **2018**, *140* (1), 94−97.

(18) Tong, W.; Gao, C.; Möhwald, H. Stable Weak Polyelectrolyte Microcapsules with pH-Responsive Permeability. *Macromolecules* **2006**, *39* (1), 335−340.

(19) Li, G.; Liu, G.; Kang, E.; Neoh, K.; Yang, X. pH-Responsive Hollow Polymeric Microspheres and Concentric Hollow Silica Microspheres from Silica− Polymer Core− Shell Microspheres. *Langmuir* **2008**, *24* (16), 9050−9055.

(20) Mauser, T.; Déjugnat, C.; Sukhorukov, G. B. Reversible pH-Dependent Properties of Multilayer Microcapsules Made of Weak Polyelectrolytes. *Macromol. Rapid Commun.* **2004**, *25* (20), 1781−1785.

(21) Wei, J.; Ju, X.-J.; Xie, R.; Mou, C.-L.; Lin, X.; Chu, L.-Y. Novel Cationic pH-Responsive poly(N,N-Dimethylaminoethyl Methacrylate) Microcapsules Prepared by a Microfluidic Technique. *J. Colloid Interface Sci.* **2011**, *357* (1), 101−108.

(22) Lee, H.; Choi, C.-H.; Abbaspourrad, A.; Wesner, C.; Caggioni, M.; Zhu, T.; Nawar, S.; Weitz, D. A. Fluorocarbon Oil Reinforced Triple Emulsion Drops. *Adv. Mater.* **2016**, *28* (38), 8425−8430.

(23) Kim, B. S.; Hrkach, J. S.; Langer, R. Synthesis and Characterization of Novel Degradable Photocrosslinked Poly(ether-Anhydride) Networks. *J. Polym. Sci., Part A: Polym. Chem.* **2000**, *38* (8), 1277−1282.

DOI: 10.1021/acs.macromol.8b00843
Macromolecules 2018, 51, 5798−5805

(24) Mathiowitz, E.; Langer, R. Polyanhydride Microspheres as Drug Carriers I. Hot-Melt Microencapsulation. *J. Controlled Release* **1987**, *5* (1), 13−22.
(25) Poetz, K. L.; Mohammed, H. S.; Snyder, B. L.; Liddil, G.; Samways, D. S. K.; Shipp, D. A. Photopolymerized Cross-Linked Thiol-Ene Polyanhydrides: Erosion, Release, and Toxicity Studies. *Biomacromolecules* **2014**, *15* (7), 2573−2582.
(26) Utada, A. S.; Lorenceau, E.; Link, D. R.; Kaplan, P. D.; Stone, H. A.; Weitz, D. A. Monodisperse Double Emulsions Generated from a Microcapillary Device. *Science* **2005**, *308* (5721), 537−541.
(27) Shah, R. K.; Shum, H. C.; Rowat, A. C.; Lee, D.; Agresti, J. J.; Utada, A. S.; Chu, L. Y.; Kim, J. W.; Fernandez-Nieves, A.; Martinez, C. J.; et al. Designer Emulsions Using Microfluidics. *Mater. Today* **2008**, *11* (4), 18−27.
(28) Duncanson, W. J.; Lin, T.; Abate, A. R.; Seiffert, S.; Shah, R. K.; Weitz, D. A. Microfluidic Synthesis of Advanced Microparticles for Encapsulation and Controlled Release. *Lab Chip* **2012**, *12* (12), 2135−2145.
(29) Yan, Q.; Zheng, H.-N.; Jiang, C.; Li, K.; Xiao, S.-J. EDC/NHS Activation Mechanism of Polymethacrylic Acid: Anhydride versus NHS-Ester. *RSC Adv.* **2015**, *5* (86), 69939−69947.
(30) Schüwer, N.; Klok, H.-A. Tuning the pH Sensitivity of Poly(methacrylic Acid) Brushes. *Langmuir* **2011**, *27* (8), 4789−4796.
(31) Ruiz-Pérez, L.; Pryke, A.; Sommer, M.; Battaglia, G.; Soutar, I.; Swanson, L.; Geoghegan, M. Conformation of Poly(methacrylic Acid) Chains in Dilute Aqueous Solution. *Macromolecules* **2008**, *41*, 2203−2211.
(32) Madsen, F. Complexation Graft Copolymer Networks: Swelling Properties, Calcium Binding and Proteolytic Enzyme Inhibition. *Biomaterials* **1999**, *20* (18), 1701−1708.
(33) Philippova, O. E.; Sitnikova, N. L.; Demidovich, G. B.; Khokhlov, A. R. Mixed Polyelectrolyte/Ionomer Behavior of Poly (Methacrylic Acid) Gel upon Titration. *Macromolecules* **1996**, *29*, 4642−4645.
(34) Philippova, O. E.; Hourdet, D.; Audebert, R.; Khokhlov, A. R. pH-Responsive Gels of Hydrophobically Modified Poly(acrylic Acid). *Macromolecules* **1997**, *30* (26), 8278−8285.
(35) Katchalsky, A.; Michaeli, I. Polyelectrolyte Gels in Salt Solutions. *J. Polym. Sci.* **1955**, *15* (79), 69−86.

DOI: 10.1021/acs.macromol.8b00843
Macromolecules 2018, 51, 5798−5805